scientific reports

Check for updates

OPEN

A method for combing multi-beam bathymetric data to correct the deep sea sub-bottom profile

Weifeng Ding[1], Xia Feng[2]✉, Na Li[1] & Yinxia Fang[1]

In the context of deep-water ocean exploration, sub-bottom profiling and multibeam bathymetric surveys are frequently integrated and synchronised to facilitate the concurrent acquisition of deep-water seafloor topography and fine sedimentary stratigraphic data. However, the complex topographic changes present in the deep ocean pose significant challenges in the exploration of the accuracy of deep-sea sub-bottom profiles. These challenges include the real-time tracking of the seafloor reflector and the splicing of profiles derived from deep-sea long-term reflection data. The accurate determination of the seafloor reflecting depth is a prerequisite for the effective correction of the data volume of deep-sea sub-bottom profiles. The development of a precise positioning and noise suppression method, namely the nearest position pair and the inverse distance weighted interpolation algorithm, has enabled the correction of the seafloor's reflecting depth and the effective splicing of sub-bottom profile data in deep water. The enhancement of the quality of deep-water sub-bottom profile data is facilitated by these processing techniques, thereby enabling the provision of a comprehensive and successively long profile for interpretation in the context of deep-water sub-bottom profile data.

Keywords Deep-sea sub-bottom profile, Multi-beam bathymetry, Seafloor reflector tracking, Profile splicing

The acoustic sub-bottom profile has been shown to play a significant role in the fields of ocean engineering and marine science in deep sea[1–3]. It has been demonstrated that it can provide insights into deep-sea geomorphological changes and the spatial structure distribution of shallow sedimentary strata, as well as revealing the shallow hazardous geologic bodies. The sub-bottom profile has also been demonstrated to be a useful tool for the study of geological sedimentary processes and tectonic activities, including seabed fluid activity, seabed stability, tectonic activity, and more[4,5]. The sub-bottom profile provides a visual high-resolution geological cross-section of tectonic sedimentation from shallow to deep sea, offering valuable insights to engineers and geologists engaged in marine engineering construction and scientific research[3,6–12].

The long-term propagation of acoustic signals in deep-sea columns exceeding 2000 m[4] has given rise to a number of unresolved issues in deep-sea sub-bottom profile, most notably the accurate tracking the seabed's reflecting event. In general, the seabed's reflecting event is tracked in real time during acquisition, and the tracked seabed's reflecting time is saved as delay parameters when recording the file after removing the propagation time in the water column. Thus, the saved raw sub-bottom data in SEG-Y format is partial underwater reflection data that removes the water column propagation[4]. However, in the presence of complex topography, such as continental slopes, ocean ridges, trenches, and seamounts, the task of accurately tracking the reflection signal of the seabed reflector becomes significantly more challenging due to the presence of high-mutation terrain. This often results in errors in the automatic tracking process, which, in turn, complicates the accurate splicing and geological interpretation of deep-sea sub-bottom profiles.

As illustrated in Fig. 1, a sub-bottom profiling section in SEG-Y format was acquired in a Pacific area with a water depth of more than 4,000 m. Figure 2 presents the seabed's reflecting curves, derived from the reflection data volume. It is evident in Fig. 2 that there are numerous abrupt jumps in the curve, which consequently results in a fragmented splicing profile as depicted in Fig. 1. The reflection events are characterised by a state of disarray, the continuity of the seabed's reflector is compromised, and the interpretation of the reflection profile becomes unfeasible. The subsequent query pertains to the methodology for accurately repositioning the reflection events within this data volume and rectifying the splicing profile. The question therefore arises as to what caused it and how to rectify it.

[1]Second Institute of Oceanography, Ministry of Natural Resources, Hangzhou 310012, China. [2]Information Engineering Institute, Hangzhou Vocational & Technical College, Hangzhou 310018, China. ✉email: fwxf1769@126.com

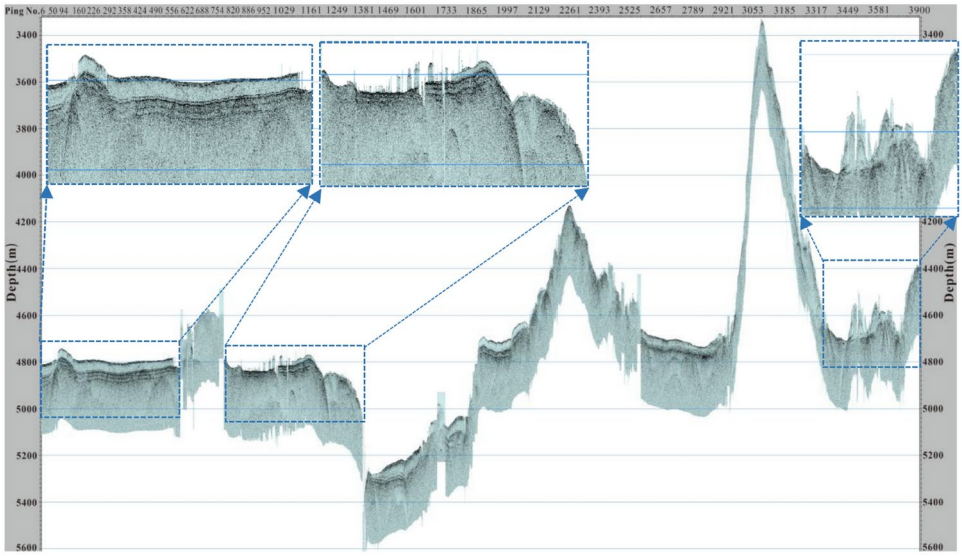


Fig. 1. Deep-sea sub-bottom profile with a depth of more than 4,000 m. (Due to numerous abrupt jumps in the topagraphy, and errous tracking of reflections from the seafloor surface in areas of abrupt terrain, the profile reflection events are characterised by a state of disarray, as illustrated in the zoomed-in figure. There are consequently results in a fragmented splicing profile. The continuity of the reflection events, especially the seabed's reflector is compromised, and the interpretation of the reflection profile becomes unfeasible.)

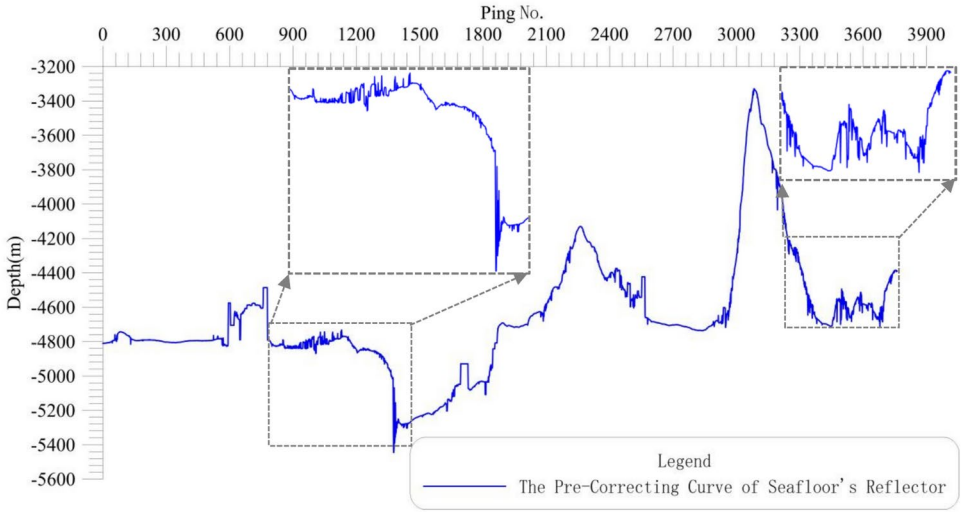


Fig. 2. The curve of tracked seafloor reflection with some abrupt jumps corresponding to Fig. 1 (The real-time tracked depth curve reveals the presence of significant interference noise in four areas over the seamount topography. There are three major instances of abrupt disturbances, especially at the steep slope of the seamount topography, where there are continuous patches of abrupt interference. Additionally, a substantial increase in noise is observed at the seamount summit, with fluctuations ranging from 50 to 150 m.)

The ship-borne deep-sea sub-bottom profile has been developed from the acoustic sub-bottom profile technology that has been utilised in shallow water, however, there are some key technological issues that must be addressed.

Firstly, an inherent conflict exists between the capacity for data recording and the storage capacity of the deep-water environment. To illustrate this, consider a seafloor depth of 2,000 m. In this scenario, the acoustic signal emitted by the ship-borne deep-sea sub-bottom profile must travel for 1.3 s to reach the seabed (calculated at a sound speed of 1,500 m/s). The acoustic transducer array requires 2.6 s to receive the reflected echo for two-way propagation. Considering the two-way propagating time in the sub-seafloor sedimentary strata, the recording time of a transmitted ping must exceed 3 s to echo back from a sub-seafloor reflector. In the event of high-sampling data being carried out, such as a sampling rate of 32 microseconds, the number of sample

points reaches 93,750, which is in excess of the storage limit of 32,767 sample points (the limit of two—bytes is $2^{15}-1=32,767$) in the standard two-byte SEG—Y format.

Secondly, the acoustic full propagation recording time is of significant concern, as it has been demonstrated to affect the emission interval. For instance, if a recording of three seconds is employed, the emission interval of the acoustic signal must exceed three seconds, as well as the reception interval. Failure to do so would result in the inability to receive the reflection data in its entirety, thereby creating an excessively large horizontal interval between Ping signals. At a minimum survey ship speed of 4 knots, the horizontal interval between Pings reaches 6 m.A larger emission interval will result in a lower signal horizontal coverage on the seafloor, which will, in turn, result in a poorer continuity of the stratigraphic reflection events. It is also important to note that the water depth has a direct impact on both the signal transmission interval and the acoustic horizontal coverage. In addition, it has been established that the ship's speed has a significant effect on the acoustic horizontal coverage. To address these challenges, some instrument manufacturers have adopted multi-Ping technology, utilising a short-time continuous emission and synchronous reception method. When receiving echoes, this method accurately tracks the seafloor's reflection, and saves parts of the reflecting data according to the track result, and removes the propagation data in the water column, thereby reducing the amount of data to be saved in SEG-Y format files. However, in actual acquisition, real-time tracking is often affected by abrupt changes in topography, and it is difficult to guarantee that all of the tracking results are accurate. Consequently, the single Ping transmitting and receiving method remains a prevalent approach in the present context.

Regardless of whether the Ping way is operated in a single or multiple mode, the seabed's reflector reflection must be tracked with a high degree of accuracy. In order to accurately determine the curve of the seafloor reflection in deep-sea sub-bottom profile data and effectively splice the related sub-bottom profile, this article explores an effective technique for correcting the tracked reflecting time of the seafloor. The method of high-precision detection of seabed topography and geomorphology using synchronously acquired multibeam bathymetric data is set out. The rectification of seabed reflection curves is further investigated, including the integration of multi-beam depth data from the same region and the subsequent completion of the splicing correction for the reflection data volume.

Solution algorithms and techniques

As demonstrated in Figs. 1 and 2, the presence of a single Ping transition also precludes the occurrence of two processing problems. Firstly, an erroneous track of seafloor reflection will directly impact the continuity of the reflecting events. Secondly, the data stored in the SEG-Y format must undergo re-splicing, as evidenced by the original profile depicted in Fig. 1. The presence of numerous interference factors during acquisition, including the pitching and rolling of the survey ship due to sea conditions, the transmitting angle and sensitivity of the instrument, and parameter settings, leads to jumping noise, as illustrated in Fig. 2. It is imperative to suppress incorrect tracking depth to prevent the rectification of a disordered sub-bottom profile. Conventional methodologies, including the sliding average method[10,13], median filtering method[14,15], and polynomial fitting method[16,17], however, are limited in their capacity to address the complexity of block-wide multi-jumping points, with the potential to compromise the integrity of nearby effective values and introduce deviations in subsequent profile splicing processing.

It is imperative to correct the seafloor's reflecting curve and calculate accurate delay recording parameters before completing the data body splice. However, in complex topographies, such as seamounts, ocean ridges, and trenches, accurately tracking the seafloor's reflector is challenging, and automatic tracking is often unreliable, necessitating manual correction. Multibeam sonar utilises a 20 kHz frequency signal to measure the depth of the seafloor, thereby generating highly accurate depth maps (e.g., 200 m grid maps). Conversely, the sub-bottom profile transmits a low frequency signal of 3.5 kHz, exhibiting a low resolution and reduced signal coverage on the seafloor. Consequently, the multibeam data can be utilised to rectify the reflectance data from the seafloor's reflector in the sub-bottom profile at the corresponding locations.

The integration of reliable data, such as high-precision multi-beam bathymetric data from specialised seabed topography surveys at the same location, with the actual data, is attempted to accurately correct the seafloor's reflecting curve and develop the delay parameter's correction technology. Finally, the sub-bottom profile splicing is implemented in an effective manner.

The nearest position pair and the inverse distance weighted interpolation algorithm

The process of correcting the seafloor's reflecting curve necessitates an accurate measurement of the seafloor depth, for which multi-beam bathymetric data is paramount. In order to effectively correct the seafloor's reflecting data and compute the delayed parameters, the objective is to utilise the precise multi-beam data from the same region. The crux of the endeavour lies in the accurate alignment of two distinct data types.

During on-site acquisition, the vessel's position remains consistent when different investigative equipment is utised on the same vessel. Consequently, the longitude and latitude in multi-beam and sub-bottom profile data can be utilised to extract the required depth, the following steps are taken. Firstly, the position data stored in the sub-bottom profile file is exported, and the position's jumping points are smoothed. Then, the positioning data of each ping is output to obtain the navigation curve in sub-bottom, as shown in Fig. 3. Subsequently, navigation data obtained from the sub-bottom profile is imported into the multi-beam bathymetric data, as illustrated in Fig. 4. This process enables the extraction of precise multi-beam bathymetry data along the specified survey position. Finally, the extracted bathymetric data is amalgamated with seafloor depth data from the sub-bottom profile reflector, and the delayed parameter for each Ping in the sub-bottom profile can be rectified.

The following methodology is proposed for the accurate fusion of the deep-sea sub-bottom profile with the multi-beam bathymetric data.



Fig. 3. The positioning curve exported from the deep sea sub-bottom profile data in a deep sea. (It is evident that there is a satisfactory degree of continuity in the actual track data derived from the sub-bottom profile, which accurately reflect the geographic location of the sub-bottom profile data in deep water.)

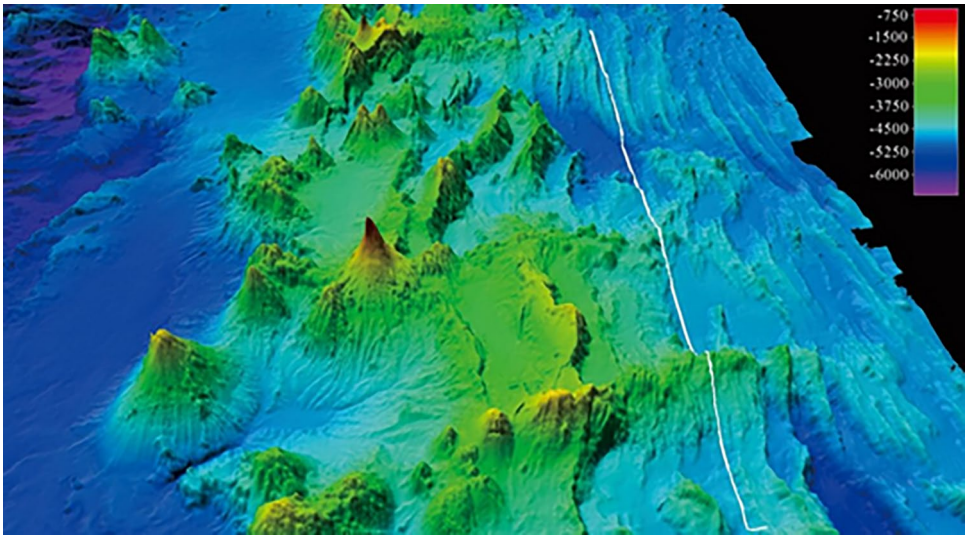


Fig. 4. The display of importing the sub-bottom profile position data (white line) into the multibeam bathymetric data to extract the accurate seafloor depth. (The navigation data of the white line, obtained from the sub-bottom profile, is imported into the multi-beam bathymetric data (the region's 3D depth colour map). This process enables the extraction of precise multi-beam bathymetry data along the specified sub-bottom profile's survey position.)

Initially, the positioning data stored in the deep-sea sub-bottom profile is smoothed. Subsequently, the positioning data from each Ping is utilised as a basis for extracting multibeam bathymetric depth.

Secondly, employing the nearest matching method, the positioning data from the sub-bottom profile is integrated into the multi-beam bathymetric data. Thereafter, the distances between the imported coordinates of the sub-bottom profile and the position in the multi-beam bathymetric data are calculated. The nearest multi-beam grid point to each imported coordinate from the sub-bottom profile is then determined. Concurrently, employing the inverse distance weighting interpolation algorithm at these nearest points, the water depth at each imported coordinate from the sub-bottom profile is computed, and the precise water depth values along the deep-sea sub-bottom profile survey line are obtained.

The calculation of precise water depth by the nearest matching method and the inverse distance weighting interpolation algorithm is a process which involves several steps.

1) Calculating the distances between each coordinate point in the deep-sea sub-bottom profile and the neighboring multibeam bathymetric grid points:

$$\mathrm{Dis}_{i,j} = \sqrt{(X_i - X_j)^2 + (Y_i - Y_j)^2}, i = 1, 2, ..., M; j = 1, 2, ..., N \tag{1}$$

In Formula (1), i denotes the index of the deep-sea sub-bottom profile positioning point, and M signifies the total number of these points. j corresponds to the index of the multibeam grid points near each deep-sea sub-bottom profile positioning point, and N indicates the total number of selected multibeam grid points participating in the calculation. The term $\mathrm{Dis}_{i,j}$ denotes the distance between each deep-sea sub-bottom profile positioning point and the neighboring multibeam grid points. The coordinates of the deep-sea sub-bottom profile positioning point are denoted by X_i and Y_i, while the coordinates of the multibeam grid point near (X_i, Y_i) are denoted by Xj and Yj.

2) Next, traversing to ascertain the minimum distance location among the multibeam bathymetric grid points for each of the sub-bottom profile position points. This is followed by the retrieval of the nearest pair of coordinates points in the multibeam bathymetric grid:

$$\mathrm{Dis}_{i,\mathrm{Min}} = \mathrm{Min}\left(\mathrm{Dis}_{i,j}\right), i = 1, 2, ..., M; j = 1, 2, ..., N \tag{2}$$

In Formula (2), $\mathrm{Dis}_{i,min}$ represents the minimum distance between each sub-bottom profile positioning point (i) and the multibeam grid points. The minimum distance searching operation is denoted by Min. The index of the deep-sea sub-bottom profile positioning point is denoted by i, and j corresponds to the index of the multibeam grid points near each i point. M and N indicate the total numbers of sub-bottom profile positioning i points and neighboring multi-beam grid j points, respectively.

3) Ultimately, the seafloor depth at the deep-sea sub-bottom profile positioning points is calculated by means of the inverse distance weighting interpolation method, based on the minimum distance points in the multibeam bathymetric data:

$$\begin{aligned} &\text{when } \mathrm{Dis}_{i,\mathrm{Min}} = 0,\ \mathrm{Depth}_i = \mathrm{Depth}_{i,\mathrm{Min}},\ i = 1, 2, \ldots, M. \\ &\text{when } \mathrm{Dis}_{i,\mathrm{Min}} > 0,\ \mathrm{Depth}_i = \sum_{j=1}^{N} \frac{\mathrm{Sum}_i - \mathrm{Dis}_{i,j}}{\mathrm{Sum}_i} \mathrm{Depth}_{i,j},\ \text{where}: \mathrm{Sum}_i = \sum_{j=1}^{N} \mathrm{Dis}_{i,j} \end{aligned} \tag{3}$$

In Formula (3), Depth_i represents the seafloor depth calculated for each of the sub-bottom profile positioning points i using the inverse distance weighting algorithm. The index of the sub-bottom profile positioning point is denoted by i, and M is the total number of positioning points. Sum_i indicates the sum of the distance from the multibeam grid points involved in the calculations for positioning point i. The total number N of multibeam grid points participating in the inverse distance weighting operation is typically set to N = 4, in which case the seafloor depth is calculated using the four points of the near multibeam grid surrounding the position point i.

In the event that the distance $\mathrm{Dis}_{i,min}$ between the sub-bottom profile positioning point i and the nearest multibeam grid point j is equal to zero, it can be deduced that positioning point i coincides with the center coordinates of multibeam grid point j, and that the seafloor depth is directly taken from the multibeam bathymetric value. Conversely, when the distance is greater than zero, the seafloor depth for sub-bottom profile positioning point i is calculated by the inverse distance weighting interpolation method.

Delay time correction for sub-bottom profile spicing

In the context of acquiring deep-sea sub-bottom profiles, real-time tracking of the seafloor reflection time is conducted during fieldwork. This enables the calculation of recording delay parameters, which consider the removal of water column propagation time to optimise the file size. Consequently, the real-time tracking outcomes of the seafloor reflection time are of paramount importance for the subsequent delay time file recording. However, it is imperative to acknowledge the presence of tracking errors, which are inevitable due to various disturbances.

In order to ensure the accuracy of the real-time tracked time of the seafloor reflection in the deep sea sub-bottom profile, the navigation data contained within the sub-bottom profile must be imported into multibeam bathymetric data to obtain accurate seafloor topography. This accurate topographic data can be used to correct the real-time tracking time of the sub-bottom profile, it involves exporting the multibeam bathymetric data and comparing it with the deep sea sub-bottom reflection data according to the navigation position(see Fig. 5),Thereafter, the difference between the two data sets is calculated. Utilising this precise discrepancy, the

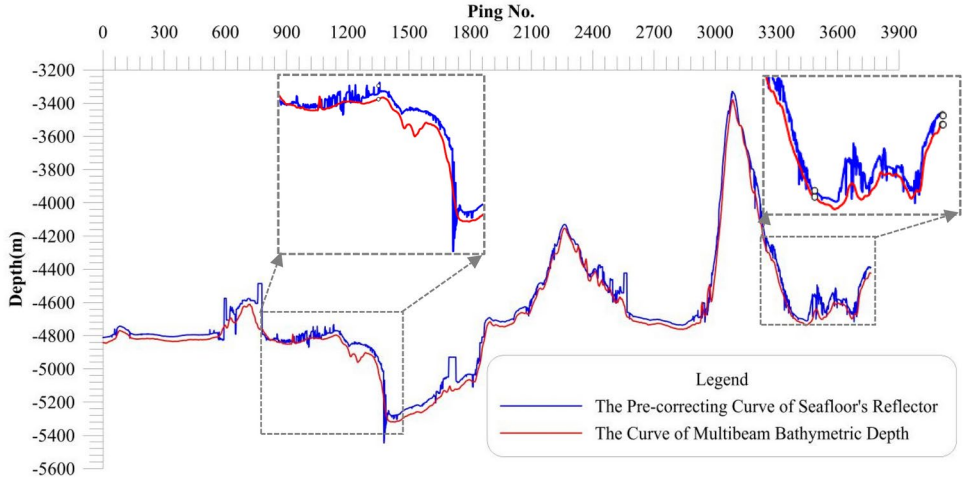


Fig. 5. Comparison of seabed depth curves between the sub-bottom profile and the multibeam bathymetric depth extracted from Fig. 4 within the same position. (Reflectance curve from sub-bottom profile is characterised by discontinuity, exhibiting patches of jumping points. This curve can be compared with multibeam bathymetry curve to analyse the actual topography.)

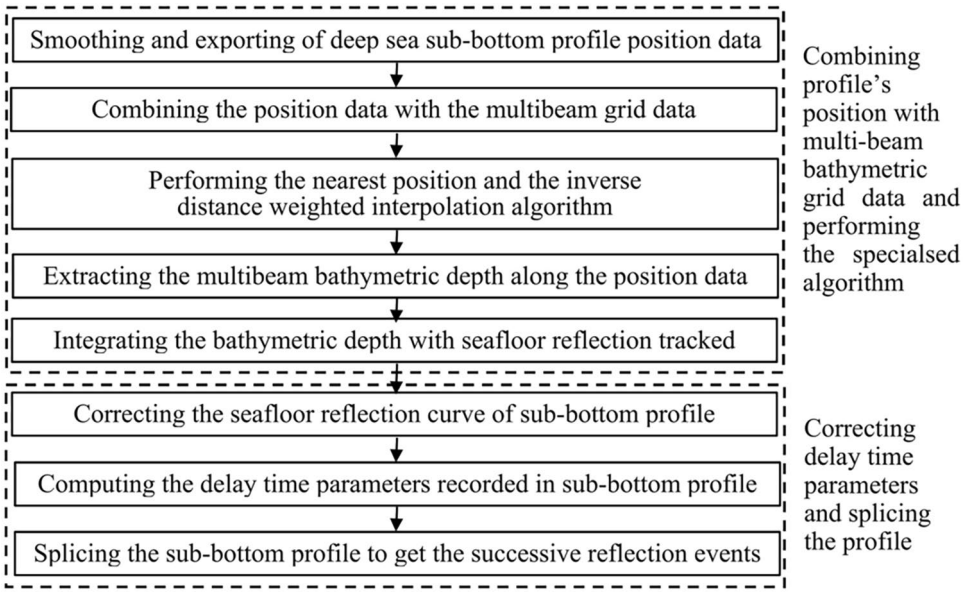


Fig. 6. Flowchart for Correcting the seafloor reflection curve and the delay time parameters in deep-Sea Sub-Bottom profile.

recording delay parameters can be meticulously calculated for each ping of the deep-sea sub-bottom profile, the profile spicing and successive mapping of the entire survey line can be conducted.

Processing workflow

As demonstrated in Fig. 6, the processing technique implemented is in accordance with the aforementioned method.

Initially, the positioning data derived from the deep-sea sub-bottom profile is extracted, and a noise reduction technique is employed to suppress field navigation data noise. This guarantees that the navigation data is aligned with the actual track of the survey vessel, thus completing the initial step of the flowchart and preparing accurate positioning data for corrections. Upon completion of the noise reduction process, the resulting positioning data is then outputted and integrated with the multi-beam bathymetric data set through the utilisation of dedicated software, thereby concluding the second step.

Subsequent to the combination of the multi-beam data with the deep-sea sub-bottom profile positioning data, the method necessitates the extraction of the multi-beam water depth profile along the positioning track. This profile is representative of the accurate seafloor topography necessary to correct the real-time tracked seafloor

reflection curve, thus completing the third step. Finally, the extracted multi-beam topographic data is compared with the tracked seafloor reflection curve to calculate the time difference, thereby providing parameters for subsequent corrections, thus completing the fourth step. The positioning data thus functions as a conduit for the integration of the deep-sea sub-bottom profile with the multi-beam topographic data, thereby facilitating the correction of time parameters for the tracking of the seafloor.

Subsequently, the processing of deep-sea sub-bottom profile time delay correction is undertaken. Initially, multi-beam bathymetric data is integrated with the tracked seafloor reflection curve. The subsequent two-way propagation of the deep-sea sub-bottom reflection data is performed, with the time difference between the actual seafloor depth and the tracking curve calculated. This process enables the rectification of any errors and the alignment of the reflection times. These steps constitute the fifth and sixth steps in the flowchart. Subsequently, the correction values for the delay time is calculated using the relationship between the tracked reflection time and the recorded raw delay time parameters. This provides accurate starting recording times for each ping in the deep sea sub-bottom data set, completing the seventh step. Finally, the reflection events of the deep sea sub-bottom reflection data are spliced together, thereby effecting a correction to the reflection data and restoring the actual profile of the reflective strata.

Processing results

The validity of this approach is substantiated by the methodology previously delineated, utilising deep-sea sub-bottom profile data from a designated offshore region, as depicted in Fig. 1. The data were collected using the Bathy-2010 system, manufactured by SyQwest, USA. The lengthy transmission intervals inherent to single ping collection, coupled with the abrupt change of topography, render the real-time tracking of seafloor reflections a challenging endeavour. As demonstrated in Fig. 2, the real-time tracked depth curve reveals the presence of significant interference noise in four areas over the seamount topography. There are three major instances of abrupt disturbances, especially at the steep slope of the seamount topography, where there are continuous patches of abrupt interference. Additionally, a substantial increase in noise is observed at the seamount summit, with fluctuations ranging from 50 to 150 m.

Whilst it is indeed possible to manually suppress large, abrupt noises, the correction of continuous patches represents a significant challenge in practice, often being time-consuming and resulting in a correction of poor quality. In order to address this issue, a multi-beam bathymetric data set and a deep-sea sub-bottom profile positioning data set were employed as intermediary variables, following the process depicted in Fig. 6. This approach yielded the intermediate outputs illustrated in Figs. 3, 4, and 5. The multi-beam depth curve was utilised to correct the tracking curve, with automatic adjustment based on statistical comparisons, yielding the outcomes depicted in Fig. 7. The corrected tracking curve is continuous and perfectly aligned with the multi-beam bathymetric curve, accurately reflecting the true topographic pattern of the seafloor bathymetry.

The efficacy of the tracking curve correction is evaluated based on the ultimate splicing outcomes of the reflection data. Subsequent to the rectification of the seafloor reflection curve, the recorded delay times for each ping are recalculated and the reflection data is spliced together, as illustrated in Fig. 8. The reflection layers in sediment-rich regions are clearly delineated, and the continuity of reflected events on seafloor and sub-layers is demonstrated to be satisfactory. The results demonstrate the preservation of the seafloor morphology, the effective mitigation of mountain interference noise, and the maintenance of continuous reflection events.

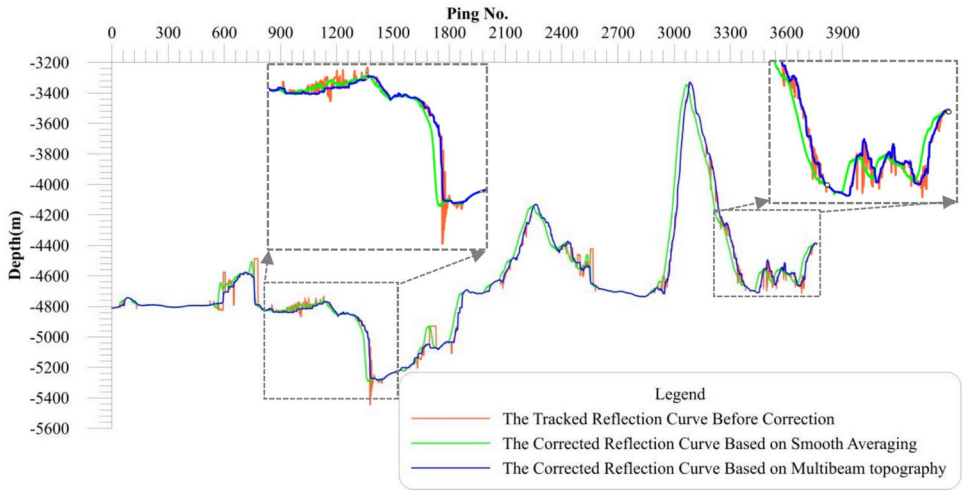


Fig. 7. The comparison of after-corrected and before-corrected seafloor reflection tracked curves based on different correction methods. (As demonstrated in the zoom window, the corrected reflection curve based on multibeam topography with blue line is more continuous than the curve based on the smooth averaging method with green line. Furthermore, the blue line accurately reflects the true topographic pattern of the seafloor bathymetry.)

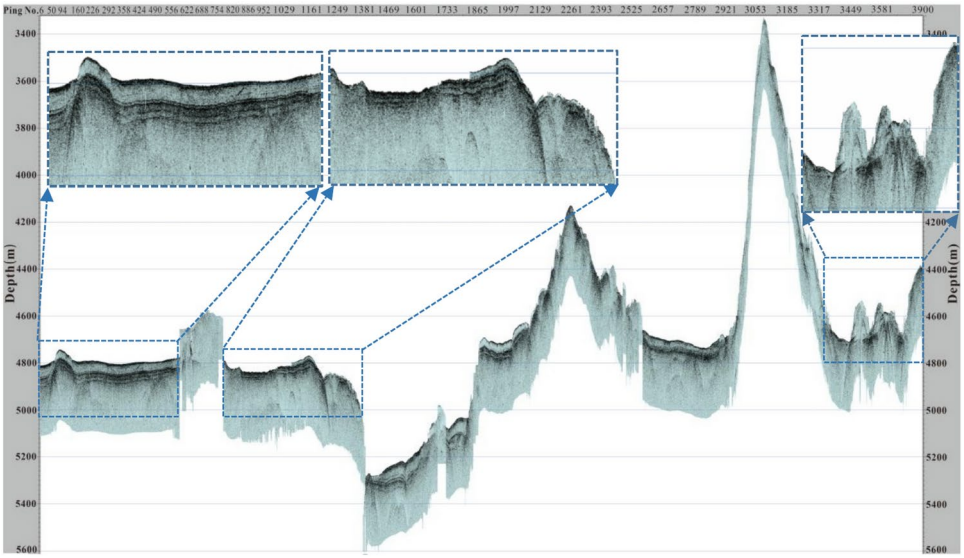


Fig. 8. Result after splicing the reflection data based on the correction curve shown in Fig. 7. (After valid correction, the reflection layers in sediment-rich regions are clearly delineated, and the continuity of reflected events on seafloor and sub-layers is demonstrated to be satisfactory.)

Conclusion

The technique of deep-sea sub-bottom profiling is employed extensively in the field of geological and geophysical surveys. Abrupt changes in seafloor depth, which can range from hundreds to thousands of metres, present a significant challenge for the real-time collection of data. Erroneous tracking of reflection data on the sub-bottom profiling seabed's reflector has been shown to have a detrimental effect on the splicing of the sub-bottom profile data body. This, in turn, has been demonstrated to have a significant impact on the generation of high-quality sub-bottom long profile result maps, as well as on the effective geological interpretation of the sub-bottom profile exploration data.

The paper proposes a methodology for the effective correction of erroneous seabed reflection tracking results in sub-bottom profile data. The proposed methodology involves the fusion of multibeam bathymetry data to correct the seabed reflection curve in the sub-bottom profile. The development of specific algorithms and technical processes has enabled the accurate splicing of sub-bottom profile reflection data bodies, which includes:

(1) The development of the nearest position pair and the inverse distance-weighted interpolation algorithm. The integration of multi-beam bathymetric depth with sub-bottom profile seafloor reflection data is achieved by utilising the nearest distance positioning data from two data sets. The inverse distance-weighted interpolation can precisely compute the seafloor depth at the deep-sea sub-bottom profile positioning points, and the difference can be accurately calculated for each ping.
(2) The correction of the delay time parameters and splicing of the sub-bottom profile. The extracted multi-beam depth is employed to correct the seafloor reflection tracking curve, after which the recorded delay times for each ping are recalculated and the reflection data is spliced together.

The methodology has been utilised for the processing of over 50,000 km of sub-bottom profile data, distributed across the South China Sea, the Pacific Ocean and the polar region. This has furnished a robust foundation for the exploration of complex seafloor subsurface layers in deep-sea environments. It is evident that the methods described in the paper require further application to real data sets and significant improvement before they can be considered fit for purpose. Furthermore, the development of comprehensive automated technology is imperative.

Data availability

All data generated or analyzed during this study are included in this published article with supplementary file.

Received: 25 November 2024; Accepted: 18 April 2025
Published online: 22 April 2025

References

1. Maroni, C. S., Quinquis, A. & Vinson, S. Horizon picking on subbottom profiles using multiresolution analysis. *Digit. Signal Process.* **11**, 269–287 (2001).
2. Fakiris, E. et al. Multi-frequency, multi-sonar mapping of shallow habitats-efficacy and management implications in the national marine park of zakynthos. *Greece. Remote Senceing.* **11**, 461. https://doi.org/10.3390/rs11040461 (2019).

3. Zhao, J., Li, S., Zhao, X. & Feng, J. A comprehensive horizon-picking method on subbottom profiles by combining envelope phase attributes, and texture analysis. *Earth & Space Sci.* https://doi.org/10.1029/2019EA000680 (2020).
4. Ding, W. et al. Technology research and development for acoustic sub-bottom survey in deep sea. *Acta Oceanol. Sin.* **37**, 70–77 (2015) ((**In Chinese**)).
5. Zhu, J. et al. High -resolution sub-bottom profiling technology using parametric array and vector hydrophone. *Appl. Acoust.* **223**, 110077 (2024).
6. Bull, J. M. et al. Design of a 3D chirp sub-bottom imaging system. *Mar. Geophys. Res.* **26**, 157–169 (2005).
7. Gutowski, M. et al. Chirp sub-bottom profiler source signature design and field testing. *Geophys. Res. Abstr.* **23**, 481–492. https://doi.org/10.1023/B:MARI.0000018247.57117.0e (2002).
8. Saleh, M. & Rabah, M. Seabed sub-bottom sediment classification using parametric sub-bottom profiler. *NRIAG J. Astron. Geophys.* **5**, 87–95 (2016).
9. Saleh, M. & Rabah, M. Seabed sub-bottom sediment classification using parametric sub-bottom profiler. *NRIAG J. Astron. & Geophys.* **5**(87), 95 (2016).
10. Kim, Y.-J. et al. A case study on swell correction of chirp sub-bottom profiler (SBP) data using multi-beam echo sounder (MBES) data. *J. Appl. Geophys.* **145**, 100–110 (2017).
11. Martin, G. et al. Three-dimensional high-resolution acoustic imaging of the sub-seabed. *Appl. Acoust.* **69**, 412–421 (2008).
12. Zhang, C. Fractal analysis of muddy submarine channel slope instability from sub-bottom profile images. *Mar. Georesour. Geotechnol.* **40**, 701–711 (2021).
13. Luo, J., Pan, G. & Ding, W. Research on processing technique of eliminating wave-induced distortion effect on sub-bottom profile. *Technical Acoustic.* **28**, 21–24 (2009) ((**In Chinese**)).
14. Wu, J., Li, C. & Zhou, W. Comparison between the noise suppressing abilities of the median filters and the average filters. *J. Nanchang Univ. (Eng. & Technol.)* **20**, 32–34 (1998) ((**In Chinese**)).
15. Ding, W., Feng, X., Fu, X., Gou, Z. & Wei, Y. Marine wave correction research on single channel seismic data and a sub-bottom profile. *Acta Oceanol. Sin.* **34**, 91–98 (2012) ((**In Chinese**)).
16. Amri, U. Recent sediment analysis, study case: Sub bottom profiler data line 8 geomarine research vessels. *J. Wetl. Environ. Manage.* **7**, 123. https://doi.org/10.20527/jwem.v7i2.171 (2019).
17. Zhang, J., Gan, X., Zhou, Z. & Yang, J. 4D track prediction of aircraft based on improved sliding window polynomial fitting method. *Adv. Aeronaut. Sci. & Eng.* **10**, 601–608 (2019) ((**In Chinese**)).

Acknowledgements

We thank the anonymous reviewers, especial reviewer 2, for their detailed comments.

Author contributions

Methodology and illustration and rivisions, Weifeng Ding; Writing – review and editing, Xia Feng; Partial translation, Na Li; Partial revision and financial support , Yinxia Fang.

Funding

This work is supported by the National Key R&D Program of China (Grants 2023YFC2808805) and the National Natural Science Foundation of China (Grants 42076083).

Declarations

Competing interests

The authors declare no competing interests.

Additional information

Supplementary Information The online version contains supplementary material available at https://doi.org/10.1038/s41598-025-99323-y.

Correspondence and requests for materials should be addressed to X.F.

Reprints and permissions information is available at www.nature.com/reprints.

Publisher's note Springer Nature remains neutral with regard to jurisdictional claims in published maps and institutional affiliations.

Open Access This article is licensed under a Creative Commons Attribution-NonCommercial-NoDerivatives 4.0 International License, which permits any non-commercial use, sharing, distribution and reproduction in any medium or format, as long as you give appropriate credit to the original author(s) and the source, provide a link to the Creative Commons licence, and indicate if you modified the licensed material. You do not have permission under this licence to share adapted material derived from this article or parts of it. The images or other third party material in this article are included in the article's Creative Commons licence, unless indicated otherwise in a credit line to the material. If material is not included in the article's Creative Commons licence and your intended use is not permitted by statutory regulation or exceeds the permitted use, you will need to obtain permission directly from the copyright holder. To view a copy of this licence, visit http://creativecommons.org/licenses/by-nc-nd/4.0/.

© The Author(s) 2025